

# **Interaction of dimeric horse cytochrome *c* with cyanide ion**

Ari Dwi Nugraheni · Satoshi Nagao · Sachiko Yanagisawa · Takashi Ogura · Shun Hirota

A. D. Nugraheni · S. Nagao · S. Hirota (✉)

Graduate School of Materials Science

Nara Institute of Science and Technology

8916-5 Takayama, Ikoma, Nara 630-0192, Japan

e-mail: [hirota@ms.naist.jp](mailto:hirota@ms.naist.jp)

S. Yanagisawa · T. Ogura

Graduate School of Life Science

University of Hyogo

3-2-1 Koto, Kamigori, Ako, Hyogo 678-1297, Japan

**Abstract** We have previously shown that methionine–heme iron coordination is perturbed in domain-swapped dimeric horse cyt *c*. To gain insight into the effect of Met dissociation in dimeric cyt *c*, we investigated its interaction with cyanide ion. We found that the Soret and Q-bands of oxidized dimeric cyt *c* at 406.5 and 529 nm red-shift to 413 and 536 nm, respectively, by an addition of 1 mM cyanide ion. The binding constant of dimeric cyt *c* with cyanide ion was obtained as  $2.5 \times 10^4 \text{ M}^{-1}$ . The Fe–CN and C–N stretching ( $\nu_{\text{Fe–CN}}$  and  $\nu_{\text{CN}}$ ) resonance Raman bands of  $\text{CN}^-$ -bound dimeric cyt *c* were observed at 443 and  $2126 \text{ cm}^{-1}$ , respectively. The  $\nu_{\text{Fe–CN}}$  frequency of dimeric cyt *c* was relatively low compared to other  $\text{CN}^-$ -bound heme proteins, and a relatively strong coupling between the Fe–C–N bending and porphyrin vibrations was observed in the  $350\text{--}450 \text{ cm}^{-1}$  region. The low  $\nu_{\text{Fe–CN}}$  frequency suggests weaker binding of the cyanide ion to dimeric cyt *c* compared to other heme proteins possessing a distal heme cavity. Although the secondary structure of dimeric cyt *c* did not change on the addition of cyanide ion according to CD measurements, the dimer dissociation rate at  $45^\circ\text{C}$  increased from  $(8.9 \pm 0.7) \times 10^{-6}$  to  $(3.8 \pm 0.2) \times 10^{-5} \text{ s}^{-1}$  with a decrease of about  $2^\circ\text{C}$  in its dissociation temperature obtained with differential scanning calorimetry. The present results show that diatomic ligands may bind to the heme iron of dimeric cyt *c* and affect its stability.

**Keywords** Cytochrome *c* · Domain swapping · Cyanide complex · Resonance Raman Spectroscopy

## Introduction

Cytochrome *c* (cyt *c*, Figure 1a) is an electron transfer heme protein in the respiratory chain of mitochondria. Cyt *c* is globular and contains three long  $\alpha$ -helices [1, 2]. Two axial ligands, His18 and Met80, are coordinated to the heme iron of cyt *c*. Met80 readily dissociates from the heme iron in oxidized cyt *c*, and instead, exogenous ligands such as cyanide ion, azide ion, imidazole, pyridine, and various other anions, have been reported to coordinate to the heme iron [3-7]. At alkaline pH, Met80 of cyt *c* has been shown to dissociate from the heme iron and instead, Lys72, -73, or -79 coordinates to the heme iron [8-11]. Cyt *c* also triggers apoptosis by an increase in peroxidase activity upon interaction with cardiolipin [12]. It has been reported that enhancement of the peroxidase activity in cyt *c* by the interaction with cardiolipin is due to the dissociation of Met80 from the heme iron [13]. According to resonance Raman and fluorescence measurements, the heme ligands of cyt *c* have been shown to exchange during unfolding and folding [14-17]. We have previously shown that horse cyt *c* forms polymers by successive domain swapping at the C-terminal helix, and Met80 dissociates from the heme iron in oligomeric cyt *c* (Figure 1b) [18, 19]. Peroxidase activity of the dimer has also been shown to increase compared to the monomer due to the dissociation of Met80 from the heme iron [20]. However, in a domain-swapped dimer of *Hydrogenobacter thermophilus* cyt *c*<sub>552</sub>, which is smaller than mammalian cyt *c* and consists of 80 amino acids,

its N-terminal  $\alpha$ -helix together with the heme was exchanged between protomers, and methionine and histidine were coordinated to the heme iron [21].

Cyanide ion forms a stable complex with the ferric heme iron in heme proteins, allowing it to be used as a probe of the active site character. Cyanide ion has been shown to bind to oxidized cyt *c* at relatively high concentration ( $\sim 50$  mM) [5, 22]. Binding of cyanide ion to cyt *c* is sensitive to the stability/flexibility of its heme region [23], and cyanide ion has been reported to bind to the alkaline isomer and acid-induced conformation of cyt *c* [24, 25]. Upon binding of cyanide ion to the heme iron in cyt *c*, the backbone of amino acid residues 77–85 have been shown to shift away from the heme, widening the heme crevice with a concomitant shift at the residues in the 50s [26].

The number of studies on domain swapping has been increasing [27-30]. It has been assumed that because the monomer and dimer share the same structures except the hinge loop, the free energy difference between the monomer and dimer in domain swapping is small, with a high energy barrier in between [21, 31, 32]. This energy barrier can be reduced by a change in pH [31], mutation in the protein [33-36], or treatment with denaturants [18, 32, 35, 37]. However, the knowledge on the factors which control the stability of domain-swapped oligomers is limited. Since the heme in dimeric cyt *c* has a water-coordination site [18], we investigated binding of cyanide ion to domain-swapped dimeric cyt *c* to gain insight into the

cyt *c*'s ligand binding properties, which may be related to its function and aggregation. We show that cyanide ion binds to the heme iron of dimeric cyt *c*, and the binding of cyanide ion accelerates dissociation of dimeric cyt *c* to monomers.

## **Materials and methods**

### **Preparation of dimeric cyt *c***

Dimeric horse cyt *c* in its oxidized state was prepared by dissolving about 100 mg of monomeric horse heart cyt *c* (Wako, Osaka, or Sigma-Aldrich) in 10 mL of 50 mM potassium phosphate buffer, pH 7.0, followed by an addition of ethanol up to 60% (v/v) at 4 °C. Cyt *c* precipitated by the addition of ethanol, and the precipitate was collected by centrifugation (8,000 g) at 4 °C for 20 min. The collected precipitate was lyophilized and subsequently dissolved in 10 mL of 50 mM potassium phosphate buffer, pH 7.0, at room temperature. After incubation at 37 °C for 60 min, the cyt *c* solution containing dimeric cyt *c* was filtrated (Millipore, pore size 0.45 µm). Dimeric cyt *c* was purified by gel chromatography (Hiload 26/60 Superdex 75, GE healthcare) using a FPLC system (BioLogic DuoFlow 10, Bio-Rad, CA) (flow rate: 0.8 mL/min, monitoring wavelength: 409 nm, solvent: 50 mM potassium phosphate buffer, pH 7.0, temperature: 4 °C). Potassium ferricyanide (Wako, Japan) (10 equivalents to the heme) was added to the dimeric cyt *c* solution. After the addition,

potassium ferricyanide was removed from the protein solution with a DE52 (Whatman, UK) column with 50 mM potassium phosphate buffer, pH 7.0. Purified dimeric cyt *c* was used immediately after purification for analyses.

To obtain the extinction coefficient of dimeric cyt *c*, we obtained the absorbance ratio of the cyt *c* solution between before-and-after dissociation of dimeric cyt *c* by heating its solution at 70 °C for 5 min. The extinction coefficient of dimeric cyt *c* (heme unit) was obtained as  $1.2 \times 10^5 \text{ M}^{-1}\text{cm}^{-1}$  at 406.5 nm using the reported extinction coefficient [38] for the monomer, which was obtained by dissociation of the dimer. The concentration of dimeric cyt *c* was adjusted with its extinction coefficient at 406.5 nm.

#### Optical absorption measurements

Binding of cyanide ion to oxidized dimeric horse cyt *c* was monitored at 20 °C with the optical absorption spectra obtained with a UV-2450 spectrophotometer (Shimadzu, Japan) using a quartz cell with a path length of 1 cm. The concentration of dimeric cyt *c* was adjusted to 10  $\mu\text{M}$  (heme unit). Potassium cyanide (Wako, Japan) was added to dimeric cyt *c* in 50 mM potassium phosphate buffer, pH 7.0 (final  $[\text{CN}^-]$ : 0.01–0.5 mM). Cyt *c* solution was incubated with cyanide ion at room temperature for 1 h before each measurement.

## Resonance Raman measurements

Resonance Raman scattering of oxidized dimeric horse cyt *c* in the presence and absence of cyanide ion were excited at 413.1 nm with an Kr<sup>+</sup> ion laser (Spectra Physics, Model 2060) at room temperature and detected with a liquid nitrogen-cooled CCD (Roper Scientific, Spec-10: 400B/LN) attached to a single polychromator (SPEX, 750M). A spinning cell was used. The slit width was set to 110  $\mu\text{m}$ . The laser power was adjusted to 1 or 5 mW at the sample point. Dimeric horse cyt *c* (25  $\mu\text{M}$ , heme unit) solution was prepared with 50 mM potassium phosphate buffer, pH 7.0. CN<sup>-</sup> complex of dimeric horse cyt *c* was obtained by an addition of potassium cyanide up to 1 mM to the dimeric cyt *c* solution. CN<sup>-</sup>-isotope complexes of dimeric cyt *c* were obtained by an addition of K<sup>13</sup>CN (ICON, <sup>13</sup>C 99 atom %) or KC<sup>15</sup>N (ICON, <sup>15</sup>N 99 atom %) to the dimeric cyt *c* solution. Raman shifts were calibrated with indene. Accuracy of the peak positions of the Raman bands was  $\pm 1\text{ cm}^{-1}$ .

## Circular dichroism (CD) measurements

CD spectra of oxidized monomeric and dimeric horse cyt *c* (10  $\mu\text{M}$ , heme unit) were measured at 20 °C with a J-725 CD spectrophotometer (Jasco, Japan) using a quartz cell with a path length of 1 mm. Monomeric and dimeric cyt *c* solutions were prepared with 50 mM potassium phosphate buffer, pH 7.0. Dimeric cyt *c* was incubated with 1 mM potassium



cyanide at room temperature for 1 h before the measurement of its  $\text{CN}^-$  complex.

#### Thermostability of dimeric cyt *c* with cyanide ion

Dissociation of oxidized dimeric horse cyt *c* in the presence and absence of 1 mM potassium cyanide was investigated by size exclusion gel chromatography (Superdex 75) using the FPLC system (BioLogic DuoFlow 10) (flow rate: 0.2 mL/min, monitoring wavelength: 412 nm, solvent: 50 mM potassium phosphate buffer, pH 7.0, temperature: 4 °C). The isosbestic wavelength (412 nm) between the absorption spectra of monomeric and dimeric cyt *c* was chosen as the monitoring wavelength. The cyt *c* solution was analyzed by gel chromatography after incubation of the solutions at 45 °C in the presence and absence of cyanide ion for 0, 1, 2, 4, and 8 h. The peak areas in the FPLC elution curves were obtained by fitting the peaks with the 100% dimer and monomer curves using the Igor Pro 6.0 program (WaveMetrics, Portland).

#### Differential scanning calorimetry (DSC) measurements

DSC thermograms of oxidized monomeric and dimeric horse cyt *c* (100  $\mu\text{M}$ , heme unit) in 50 mM potassium phosphate buffer, pH 7.0, were measured in the presence and absence of 1 mM potassium cyanide with a VP-DSC calorimeter (GE Healthcare). The protein solution was

degassed for 2–3 minutes at 25 °C before measurements. DSC scan rate was 1 °C/min.

## Results

### Optical absorption spectra of dimeric cyt *c* in the presence of cyanide ion

The Soret band of oxidized dimeric horse cyt *c* at 406.5 nm red-shifted to 413 nm by an addition of cyanide ion, and the shift was completed at about 1 mM cyanide ion (Figure 2A).

The Q band at 529 nm of oxidized dimeric cyt *c* also red-shifted to 536 nm by the addition of cyanide ion (Figure S1). Although it is known that cyanide ion binds to monomeric cyt *c* at a high cyanide ion concentration of about 50 mM, causing similar red-shifts in the Soret and Q bands [3, 5, 6], no significant change was observed in the absorption spectrum of monomeric cyt *c* by an addition of 1 mM cyanide ion (Figure S2). Difference absorption spectra were calculated by subtracting the spectrum of dimeric cyt *c* in the absence of cyanide ion from the spectra in the presence of it. Negative and positive peaks were observed at 402 and 417 nm, respectively, in the difference spectra with an isosbestic point at 410.6 nm (Figure 2A, Inset). These results indicate that cyanide ion binds to the heme iron in dimeric cyt *c* at cyanide concentrations lower than that necessary for binding to monomeric cyt *c*, due to dissociation of methionine from the heme iron in the dimer.

## Resonance Raman spectra of CN<sup>-</sup>-complex of dimeric cyt *c*

Resonance Raman scattering of oxidized dimeric horse cyt *c* were excited at 413.1 nm in the presence and absence of 1 mM cyanide ion (Figure 3). The  $\nu_2$  (spin-state marker),  $\nu_3$  (coordination-number marker), and  $\nu_4$  (oxidation-state marker) bands [39-42] were observed at 1586, 1504, and 1373 cm<sup>-1</sup>, respectively, in the Raman spectrum of dimeric cyt *c* in the absence of cyanide ion (Figure 3A, curve a). These frequencies were characteristic of the spectra of 6-coordinate ferric low spin species. Small or no change was observed in the frequencies of the  $\nu_2$  (1587 cm<sup>-1</sup>),  $\nu_3$  (1504 cm<sup>-1</sup>), and  $\nu_4$  (1373 cm<sup>-1</sup>) bands by the addition of 1 mM cyanide ion, showing that dimeric cyt *c* maintained the 6-coordinate ferric low spin character in the presence of cyanide ion (Figure 3A, curve b).

Resonance Raman spectra of oxidized dimeric horse cyt *c* in the presence of 1 mM <sup>12</sup>C<sup>14</sup>N<sup>-</sup>, <sup>13</sup>C<sup>14</sup>N<sup>-</sup>, or <sup>12</sup>C<sup>15</sup>N<sup>-</sup> in the low and high frequency regions exhibited isotope-sensitive bands (Figures 3B and 3C). In the low frequency region, the band at 443 cm<sup>-1</sup> observed for <sup>12</sup>C<sup>14</sup>N<sup>-</sup>-bound dimeric cyt *c* down-shifted to 440 cm<sup>-1</sup> for the <sup>13</sup>C<sup>14</sup>N<sup>-</sup> and <sup>12</sup>C<sup>15</sup>N<sup>-</sup> complexes. We assigned this band to the Fe–CN stretching ( $\nu_{\text{Fe–CN}}$ ) mode of the cyanide ion bound to dimeric cyt *c*, showing that the cyanide ion binds to the heme iron of dimeric cyt *c*. The difference spectrum between the spectra of <sup>12</sup>C<sup>14</sup>N<sup>-</sup>- and <sup>13</sup>C<sup>14</sup>N<sup>-</sup>-bound dimeric cyt *c* exhibited peaks around 350 to 450 cm<sup>-1</sup>, whereas the intensity of these peaks decreased

significantly in the difference spectrum between the spectra of  $^{12}\text{C}^{14}\text{N}^-$ - and  $^{12}\text{C}^{15}\text{N}^-$ -bound dimeric cyt *c*, except for the peaks around 440–450  $\text{cm}^{-1}$  (Figure 3B, curves d and e). These properties in the difference Raman spectra are characteristic of the spectra of  $\text{CN}^-$ -bound heme proteins, in which the Fe–C–N bending ( $\delta_{\text{FeCN}}$ ) mode couples with porphyrin vibrational modes [43, 44]. The bands of ferric cyt *c* at 349, 359, 380, 397, and 412/418  $\text{cm}^{-1}$  have been assigned to porphyrin  $\nu_8$ ,  $\nu_{50}$ , propionate bending, cysteine side chain bending, and ethyl bending modes, respectively [42, 45]. We may assign the  $\text{CN}^-$ -bound dimeric cyt *c* bands at 343, 371 and 393  $\text{cm}^{-1}$  to  $\nu_8$ , heme propionate bending, and cysteine side chain bending modes, respectively. The heme propionate and cysteine side chain bending modes seem to vibrationally couple with the  $\delta_{\text{FeCN}}$  mode in  $\text{CN}^-$ -bound dimeric cyt *c*, whereas the in-plane symmetric  $\nu_8$  mode seems not to couple with the  $\delta_{\text{FeCN}}$  mode.

In the high frequency region, positive and negative peaks at 2126 and 2078  $\text{cm}^{-1}$ , respectively, were observed in the difference spectrum between the spectra of  $^{12}\text{C}^{14}\text{N}^-$ - and  $^{13}\text{C}^{14}\text{N}^-$ -bound dimeric cyt *c* (Figure 3C). These frequencies are in good agreement with the C–N stretching ( $\nu_{\text{CN}}$ ) frequencies of  $\text{CN}^-$ -bound myoglobin (Mb) observed with IR [46] and resonance Raman ( $^{12}\text{C}^{14}\text{N}^-$ -bound Mb; 2127  $\text{cm}^{-1}$ ) measurements [43], and we assign this band to the  $\nu_{\text{CN}}$  mode of  $\text{CN}^-$ -bound dimeric cyt *c*.

### Secondary structure of dimeric cyt *c* in the presence of cyanide ion

The CD spectrum of dimeric cyt *c* exhibited negative peaks at 209 and 222 nm, which were characteristic of an  $\alpha$ -helical structure (Figure 4). Small changes in the intensities of the 209- and 222-nm negative peaks were observed compared to the spectrum of its monomer, due to the structural change at the hinge loop [18]. However, the CD spectrum of dimeric cyt *c* did not change by an addition of 1 mM cyanide ion, showing that the secondary structure of dimeric cyt *c* was not affected by binding of the cyanide ion to the heme.

### Effect of cyanide ion on dissociation of dimeric cyt *c*

Dissociation of oxidized dimeric horse cyt *c* to monomers in the presence and absence of cyanide ion was monitored by size exclusion gel chromatography (Figure 5). Dimeric cyt *c* dissociated to monomers at 45 °C with a rate constant of  $(8.9 \pm 0.7) \times 10^{-6} \text{ s}^{-1}$ , whereas the rate constant increased about 4 times in the presence of 1 mM cyanide ion  $((3.8 \pm 0.2) \times 10^{-5} \text{ s}^{-1})$ . These results show that binding of cyanide ion to the heme iron accelerates dissociation of dimeric cyt *c*. The interaction between the protomers in dimeric cyt *c* may become weaker by the binding of the cyanide ion due to steric repulsions between the bound cyanide ion and protein surrounding. Upon dissociation of dimeric cyt *c* to monomers, the Soret band shifted back to 409 nm and the intensity of the 695-nm band characteristic for the Met-heme

coordination recovered (Figure S3), showing that the cyanide ion dissociated from the heme when the dimer dissociated to monomers.

DSC thermograms of oxidized dimeric horse cyt *c* were measured in the presence and absence of 1 mM cyanide ion to investigate the effect of cyanide ion on protein stability (Figure 6). A negative peak was observed around 58 °C in the thermogram of dimeric cyt *c*, whereas no peak was observed in that of the monomer. The peak temperature ( $T_m$ ) represents the dissociation temperature of dimeric cyt *c* to monomers, and the peak area corresponds to the enthalpy change ( $\Delta H$ ) upon the dissociation.  $T_m$  was obtained as  $58.4 \pm 0.4$  °C for dimeric cyt *c* and decreased to  $56.6 \pm 0.2$  °C by an addition of 1 mM cyanide ion, showing that the dissociation temperature of dimeric cyt *c* decreases by the addition of cyanide ion. These results were in agreement with the results of size exclusion gel chromatography, showing that cyanide ion accelerates dissociation of dimeric cyt *c*. However, the  $\Delta H$  value was obtained as  $-40.0 \pm 2$  kcal/mol in the absence of cyanide ion as previously reported [18], and changed to  $-21.0 \pm 2$  kcal/mol by the addition of 1 mM cyanide ion.

## Discussion

The binding constant of cyanide ion to dimeric cyt *c* was obtained to estimate its cyanide affinity. We defined  $\Delta\Delta\text{Abs}$  as the difference between the absorption changes at 402 and 413

nm upon the cyanide ion binding, and  $\Delta\Delta\epsilon$  as that between the absorption coefficient changes at 402 and 413 nm upon binding. The  $\Delta\Delta\text{Abs}$  values obey the following equation [47]:

$$\Delta\Delta\text{Abs} = \Delta\Delta\epsilon l / 2 \times \{([dimeric\ cyt\ c] + [CN^-] + 1/K_i) - \{([dimeric\ cyt\ c] + [CN^-] + 1/K_i)^2 - 4[dimeric\ cyt\ c][CN^-]\}^{0.5}\} \quad (1)$$

where  $l$  represents the cell path length, and  $[cyt\ c]$  and  $[CN^-]$  represent the concentrations of *cyt c* and cyanide ion, respectively.  $K_i$  represents the association constant between dimeric *cyt c* (heme unit) and the cyanide ion. The values of  $\Delta\Delta\epsilon$  and  $K_i$  were obtained by least-square fitting the plot of  $\Delta\Delta\text{Abs}$  vs  $[CN^-]$  with eq. 1 (Figure 2B). The binding constant of dimeric *cyt c* with cyanide ion was obtained as  $2.5 \times 10^4\ M^{-1}$ , whereas the binding constant of ferric Mb with cyanide ion has been reported as  $1.4 \times 10^7\ M^{-1}$  [48]. The binding constant of dimeric *cyt c* with cyanide ion was about 1/1000 that of Mb, presumably because *cyt c* lacks a distal heme cavity and the bound cyanide ion suffers steric hinderance from the protein surrounding.

Although the  $\nu_{CN}$  frequency of  $CN^-$ -bound dimeric *cyt c* was very close to those of other  $CN^-$ -bound heme proteins [43, 46, 49], its  $\nu_{Fe-CN}$  frequency was lower than those observed in other  $CN^-$ -bound heme proteins, such as Mb, hemoglobin (Hb), and horse radish peroxidase ( $452\text{--}454\ cm^{-1}$ ) (Figures 3B and 3C) [43, 50-52]. These results indicate a weaker binding of

cyanide ion to the heme in dimeric cyt *c* compared to other heme proteins, which is in agreement with the smaller binding constant for the CN<sup>-</sup> complex of dimeric cyt *c* compared to Mb.

The Fe–C–N unit is linear and cyanide ion favors binding perpendicular to the heme plane in model compounds according to X-ray crystal analyses [53]. The Fe–C–N unit is approximately linear in CN<sup>-</sup>-bound monomeric ferric horse cyt *c* (Fe–C–N angle of 177°) (PDB: 1I5T) [26]. The approximately linear structure of the Fe–C–N unit has also been detected in several CN<sup>-</sup>-bound heme proteins, including Mb (Fe–C–N angle of 166°) (PDB: 1EBC) [54] and nitrophorin (Fe–C–N angle of 173°) (PDB: 3NP1) [55]. However, in *Chlamydomonas* hemoglobin, the Fe–C–N structure is highly distorted in a bent structure (Fe–C–N angle of 130°) with a hydrogen bond formed between the cyanide ion and the glutamine side chain in the heme pocket (PDB: 1DLY) [56], and the  $\nu_{\text{Fe-CN}}$  band has been detected at a relatively low frequency, 440 cm<sup>-1</sup> [57]. It has been reported that when the Fe–C–N unit adopts a bent structure, the  $\nu_{\text{Fe-CN}}$  and  $\delta_{\text{FeCN}}$  modes are vibrationally mixed with each other, and both modes of the <sup>13</sup>C<sup>14</sup>N<sup>-</sup> adduct exhibit larger frequency shifts from those of the <sup>12</sup>C<sup>14</sup>N<sup>-</sup> adduct compared to the frequency shifts observed for the <sup>12</sup>C<sup>15</sup>N<sup>-</sup> adduct [58]. However, the frequency shift of the  $\nu_{\text{Fe-CN}}$  band of <sup>13</sup>C<sup>14</sup>N<sup>-</sup>-bound dimeric cyt *c* from that of the <sup>12</sup>C<sup>14</sup>N<sup>-</sup> adduct was similar to the shift observed for the <sup>12</sup>C<sup>15</sup>N<sup>-</sup> adduct (Figure 3B). These



results indicate that the Fe-C-N unit in dimeric cyt *c* also adopts a relatively linear conformation. CN<sup>-</sup>-bound ferric myoglobin has been shown to exhibit a Fe-C-N angle of 166° with a hydrogen bond between the bound cyanide ion and the imidazole ring of the distal histidine (PDB: 1EBC) [54]. It has been reported that Tyr67 forms a hydrogen bond with the bound cyanide ion in CN<sup>-</sup>-bound ferric Met80Ala yeast iso-1 cyt *c* [59-61] and horse cyt *c* [26]. From the crystal structure of dimeric cyt *c* (PDB: 3NBS), Tyr67 is also the nearest amino acid to the heme. Therefore, Tyr67 may create a hydrogen bond with the cyanide ion in dimeric horse cyt *c*.

It has been shown that the side chains of the aromatic residues in the distal pocket of CN<sup>-</sup>-bound ferric Met80Ala yeast iso-1-cyt *c* exhibit similar orientations to those of wild-type yeast iso-1-cyt *c* [59], whereas amino acid residues 77–85 in CN<sup>-</sup>-bound ferric horse cyt *c* shifts away from the heme with a widening of the heme crevice compared to its native ferric form due to the steric interaction between the bound cyanide ion and the long side chain of Met80 [26]. The side chain of Phe82 is also located relatively close to the heme in dimeric cyt *c* (PDB: 3NBS). Therefore, the steric interaction may exist between the bound cyanide ion and its protein surrounding region containing Met80 and Phe82 in CN<sup>-</sup>-bound dimeric cyt *c*, and enhance dissociation of the dimer to monomers.

There was no significant change in the secondary structure of dimeric cyt *c* by the

addition of cyanide ion according to the CD spectra (Figure 4), although cyanide ion was bound to the heme in  $\text{CN}^-$ -bound dimeric cyt *c* according to resonance Raman measurements (Figure 3). These results show that the  $\alpha$ -helices of the dimer did not unfold by the binding of cyanide ion. The change in  $\Delta H$  on dissociation of dimeric cyt *c* to monomers became smaller by the addition of cyanide ion according to the DSC measurements (Figure 6), indicating that dimeric cyt *c* was enthalpically stabilized by the cyanide binding to the heme iron. Although dimeric cyt *c* was stabilized by coordination of a cyanide ion to the heme iron, dissociation of dimeric cyt *c* to monomers became faster and  $T_m$  for the dissociation decreased by about 2 °C by the addition of cyanide ion (Figures 5 and 6). Therefore, the activation energy of dimer dissociation may decrease due to the interaction of cyanide ion with the protein surrounding in the dimer. In fact, a structural change has been shown to occur on binding of cyanide ion to monomeric cyt *c*, in which the backbone of amino acid residues 77–85 of cyt *c* shifts away from the heme with a widening of the heme crevice [26]. Although cyanide binding did not cause a large change in the protein structure of dimeric cyt *c*, the bound cyanide ion interacted with the protein surrounding and accelerated the dissociation of the dimer.

**Acknowledgement** We thank Mr. Leigh McDowell, Nara Institute of Science and Technology, for his advice on manuscript preparation. This work was partially supported by

Grants-in-Aid for Scientific Research from MEXT (Priority Areas, No. 23107723 (S.H.)), JSPS (Category B No.21350095 (S.H.)), Sankyo Foundation of Life Science (S.H.), and Toray Science Foundation (S.H.).

## References

1. Dickerson RE, Takano T, Eisenberg D, Kallai OB, Samson L, Cooper A, Margoliash E (1971) *J. Biol. Chem.* 246:1511–1535
2. Bushnell GW, Louie GV, Brayer GD (1990) *J. Mol. Biol.* 214:585–595
3. Horecker BL, Kornberg A (1946) *J. Biol. Chem.* 165:11–20
4. Horecker BL, Stannard JN (1948) *J. Biol. Chem.* 172:589–597
5. Tsou CL (1952) *Biochem. J.* 50:493–499
6. Butt WD, Keilin D (1962) *Proc. R. Soc. Lond. B* 156:429–458
7. Sutin N, Yandell JK (1972) *J. Biol. Chem.* 247:6932–6936
8. Rosell FI, Ferrer JC, Mauk AG (1998) *J. Am. Chem. Soc.* 120:11234–11245
9. Pollock WB, Rosell FI, Twitchett MB, Dumont ME, Mauk AG (1998) *Biochemistry* 37:6124–6131
10. Banci L, Bertini I, Spyroulias GA, Turano P (1998) *Eur. J. Inorg. Chem.* 5:583–591
11. Ying T, Zhong F, Xie J, Feng Y, Wang ZH, Huang ZX, Tan X (2009) *J. Bioenerg. Biomembr.* 41:251–257

12. Kagan VE, Tyurin VA, Jiang J, Tyurina YY, Ritov VB, Amoscato AA, Osipov AN, Belikova NA, Kapralov AA, Kini V, Vlasova, II, Zhao Q, Zou M, Di P, Svistunenko DA, Kurnikov IV, Borisenko GG (2005) *Nat. Chem. Biol.* 1:223-232
13. Belikova NA, Vladimirov YA, Osipov AN, Kapralov AA, Tyurin VA, Potapovich MV, Basova LV, Peterson J, Kurnikov IV, Kagan VE (2006) *Biochemistry* 45:4998–5009
14. Takahashi S, Yeh SR, Das TK, Chan CK, Gottfried DS, Rousseau DL (1997) *Nat. Struct. Biol.* 4:44–50
15. Yeh SR, Takahashi S, Fan B, Rousseau DL (1997) *Nat. Struct. Biol.* 4:51–56
16. Yeh SR, Han SW, Rousseau DL (1998) *Acc. Chem. Res.* 31:727–736
17. Yeh SR, Rousseau DL (1999) *J. Biol. Chem.* 274:17853–17859
18. Hirota S, Hattori Y, Nagao S, Taketa M, Komori H, Kamikubo H, Wang Z, Takahashi I, Negi S, Sugiura Y, Kataoka M, Higuchi Y (2010) *Proc. Natl. Acad. Sci. U.S.A.* 107:12854–12859
19. Hirota S, Ueda M, Hayashi Y, Nagao S, Kamikubo H, Kataoka M (2012) *J. Biochem.* 152:521–529
20. Wang Z, Matsuo T, Nagao S, Hirota S (2011) *Org. Biomol. Chem.* 9:4766–4769
21. Hayashi Y, Nagao S, Osuka H, Komori H, Higuchi Y, Hirota S (2012) *Biochemistry* 51:8608–8616

22. George P, Glauser SC, Schejter A (1967) *J. Biol. Chem.* 242:1690–1695
23. Varhač R, Tomášková N, Fabián M, Sedlák E (2009) *Biophys. Chem.* 144:21–26
24. Filosa A, Ismail AA, English AM (1999) *J. Biol. Inorg. Chem.* 4:717–726
25. Varhač R, Antalík M (2008) *J. Biol. Inorg. Chem.* 13:713–721
26. Yao Y, Qian C, Ye K, Wang J, Bai Z, Tang W (2002) *J. Biol. Inorg. Chem.* 7:539–547
27. Newcomer ME (2002) *Curr. Opin. Struct. Biol.* 12:48–53
28. Rousseau F, Schymkowitz JW, Itzhaki LS (2003) *Structure* 11:243–251
29. Liu Y, Eisenberg D (2002) *Protein Sci.* 11:1285–1299
30. Bennett MJ, Sawaya MR, Eisenberg D (2006) *Structure* 14:811–824
31. Bennett MJ, Choe S, Eisenberg D (1994) *Proc. Natl. Acad. Sci. U.S.A.* 91:3127–3131
32. Bennett MJ, Schlunegger MP, Eisenberg D (1995) *Protein Sci.* 4:2455–2468
33. Rousseau F, Schymkowitz JW, Wilkinson HR, Itzhaki LS (2001) *Proc. Natl. Acad. Sci. U.S.A.* 98:5596–5601
34. Schymkowitz JW, Rousseau F, Wilkinson HR, Friedler A, Itzhaki LS (2001) *Nat. Struct. Biol.* 8:888–892
35. Barrientos LG, Louis JM, Botos I, Mori T, Han Z, O'Keefe BR, Boyd MR, Wlodawer A, Gronenborn AM (2002) *Structure* 10:673–686
36. Chen YW, Stott K, Perutz MF (1999) *Proc. Natl. Acad. Sci. U.S.A.* 96:1257–1261

37. Liu Y, Gotte G, Libonati M, Eisenberg D (2002) *Protein Sci.* 11:371–380
38. Margoliash E, Frohwirt N, Wiener E (1959) *Biochem. J.* 71:559–1570
39. Kitagawa T, Kyogoku Y, Iizuka T, Saito MI (1976) *J. Am. Chem. Soc.* 98:5169–5173
40. Spiro TG, Burke JM (1976) *J. Am. Chem. Soc.* 98:5482–5489
41. Kitagawa T, Hirota S (2002) In: Chalmers JM, Griffiths PR (eds) *Handbook of Vibrational Spectroscopy*. John Wiley & Sons Ltd., Chichester, pp. 3426–3446
42. Hu SZ, Morris IK, Singh JP, Smith KM, Spiro TG (1993) *J. Am. Chem. Soc.* 115:12446–12458
43. Hirota S, Ogura T, ShinzawaItoh K, Yoshikawa S, Kitagawa T (1996) *J. Phys. Chem.* 100:15274–15279
44. Maes EM, Walker FA, Montfort WR, Czernuszewicz RS (2001) *J. Am. Chem. Soc.* 123:11664–11672
45. Abe M, Kitagawa T, Kyogoku Y (1978) *J. Chem. Phys.* 69:4526–4534
46. Yoshikawa S, O'Keeffe DH, Caughey WS (1985) *J. Biol. Chem.* 260:3518–3528
47. Hirota S, Hayamizu K, Okuno T, Kishi M, Iwasaki H, Kondo T, Hibino T, Takabe T, Kohzuma T, Yamauchi O (2000) *Biochemistry* 39:6357–6364
48. Schejter A, Plotkin B (1988) *Biochem. J.* 255:353–356
49. Reddy KS, Yonetani T, Tsuneshige A, Chance B, Kushkuley B, Stavrov SS, Vanderkooi

- JM (1996) *Biochemistry* 35:5562–5570
50. Yu NT, Benko B, Kerr EA, Gersonde K (1984) *Proc. Natl. Acad. Sci. U.S.A.* 81:5106–5110
51. Henry ER, Rousseau DL, Hopfield JJ, Noble RW, Simon SR (1985) *Biochemistry* 24:5907–5918
52. Sitter AJ, Reczek CM, Turner J (1985) *Biochim. Biophys. Acta* 828:229–235
53. Scheidt WR, Lee YJ, Luangdilok W, Haller KJ, Anzai K, Hatano K (1983) *Inorg. Chem.* 22:1516–1522
54. Bolognesi M, Rosano C, Losso R, Borassi A, Rizzi M, Wittenberg JB, Boffi A, Ascenzi P (1999) *Biophys. J.* 77:1093–1099
55. Weichsel A, Andersen JF, Champagne DE, Walker FA, Montfort WR (1998) *Nat. Struct. Biol.* 5:304–309
56. Pesce A, Couture M, Dewilde S, Guertin M, Yamauchi K, Ascenzi P, Moens L, Bolognesi M (2000) *EMBO J.* 19:2424–2434
57. Das TK, Couture M, Guertin M, Rousseau DL (2000) *J. Phys. Chem. B* 104:10750–10756
58. Simianu MC, Kincaid JR (1995) *J. Am. Chem. Soc.* 117:4628–4636
59. Banci L, Bertini I, Bren KL, Gray HB, Sompornpisut P, Turano P (1995) *Biochemistry*

34:11385-11398

60. Bren KL, Gray HB, Banci L, Bertini I, Turano P (1995) *J. Am. Chem. Soc.*

117:8067–8073

61. Ying T, Wang ZH, Lin YW, Xie J, Tan X, Huang ZX (2009) *Chem.*

*Commun.*:4512–4514



## Figure Legends

**Fig. 1** Structures of monomeric (**A**) (PDB:1HRC) and dimeric (**B**) (PDB:3NBS) horse cyt *c*.

Each protomer in dimeric cyt *c* is depicted in red and blue. The hemes, His18, and Met80 are shown as stick models in gray, green, and yellow colors, respectively. The N- and C-termini and the N- and C-terminal helices are labeled as N, C,  $\alpha$ N, and  $\alpha$ C, respectively.

**Fig. 2** Changes in the absorption spectra of oxidized dimeric horse cyt *c* by an addition of cyanide ions. **A** Absorption spectra in the 250–800-nm region. *Inset*: Different absorption spectra between the spectra of dimeric cyt *c* in the presence of cyanide ion subtracted with that in the absence of it. Measurement conditions: dimeric cyt *c* concentration (heme unit): 10  $\mu$ M, KCN concentration: 0, 0.01, 0.025, 0.05, 0.1, 0.15, 0.2, 0.3, 0.4 and 0.5 mM, solvent: 50 mM potassium phosphate buffer, pH 7.0, temperature: 20 °C. **B** Plot of  $\Delta\Delta$ Abs vs  $[\text{CN}^-]$ , together with the least-square fitted curve according to eq. 1.

**Fig. 3** Resonance Raman spectra of oxidized dimeric horse cyt *c*. **A** Resonance Raman spectra of dimeric cyt *c* in the absence (*a*) and presence (*b*) of 1 mM cyanide ion. **B** Resonance Raman spectra of  $^{12}\text{C}^{14}\text{N}^-$  (*a*),  $^{13}\text{C}^{14}\text{N}^-$  (*b*), and  $^{12}\text{C}^{15}\text{N}^-$ -bound (*c*) dimeric cyt *c* in the low frequency region and their difference spectra,  $^{12}\text{C}^{14}\text{N}^-$  minus  $^{13}\text{C}^{14}\text{N}^-$  adducts (*d*) and  $^{12}\text{C}^{14}\text{N}^-$

minus  $^{12}\text{C}^{15}\text{N}^-$  (*e*) adducts. **C** Resonance Raman spectra of  $^{12}\text{C}^{14}\text{N}^-$  - (*a*) and  $^{13}\text{C}^{14}\text{N}^-$ -bound (*b*) dimeric cyt *c* in the high frequency region and their difference spectrum,  $^{12}\text{C}^{14}\text{N}^-$  minus  $^{13}\text{C}^{14}\text{N}^-$  adducts (*c*). The intensities of the difference spectra are expanded three times. Measurement conditions: dimeric cyt *c* concentration (heme unit): 20  $\mu\text{M}$ , KCN concentration: 1 mM, solvent: 50 mM potassium phosphate buffer, pH 7.0, laser power: (A, B) 1 mW, (C) 5 mW, accumulation: (A, B) 15 min, (C) 40 min, temperature: room temperature.

**Fig. 4** CD spectra of oxidized monomeric and dimeric horse cyt *c* in the presence and absence of cyanide ion: (black) Monomeric cyt *c*; (red) dimeric cyt *c*; (blue) dimeric cyt *c* in the presence of cyanide ion. Measurement conditions: protein concentration (heme unit): 10  $\mu\text{M}$ ; KCN concentration: 1 mM, solvent: 50 mM potassium phosphate buffer, pH 7.0, temperature: 25 °C.

**Fig. 5** Dissociation of dimeric cyt *c* by incubation at 45 °C in the absence (square) and presence (circle) of 1 mM cyanide ion. The ratio of dimeric cyt *c* was estimated from the peak areas in the elution curves of size exclusion chromatography after the incubation. Least-square fitted exponential curves are overlapped. Incubation conditions: dimeric cyt *c*

concentration (heme unit): 100  $\mu$ M, solvent: 50 mM potassium phosphate buffer, pH 7.0, incubation time: 0, 1, 2, 4, and 8 h. Measurement conditions: flow rate: 0.2 mL/min, monitoring wavelength: 412 nm, solvent: 50 mM potassium phosphate buffer, pH 7.0, temperature: 4  $^{\circ}$ C.

**Fig. 6** DSC thermograms of monomeric and dimeric cyt *c*: (black) Monomeric cyt *c*; (red) dimeric cyt *c*; (blue) dimeric cyt *c* in the presence of cyanide ion. Measurement conditions: cyt *c* concentration (heme unit): 100  $\mu$ M, KCN concentration: 0.1 mM, solvent: 50 mM potassium phosphate buffer, pH 7.0.

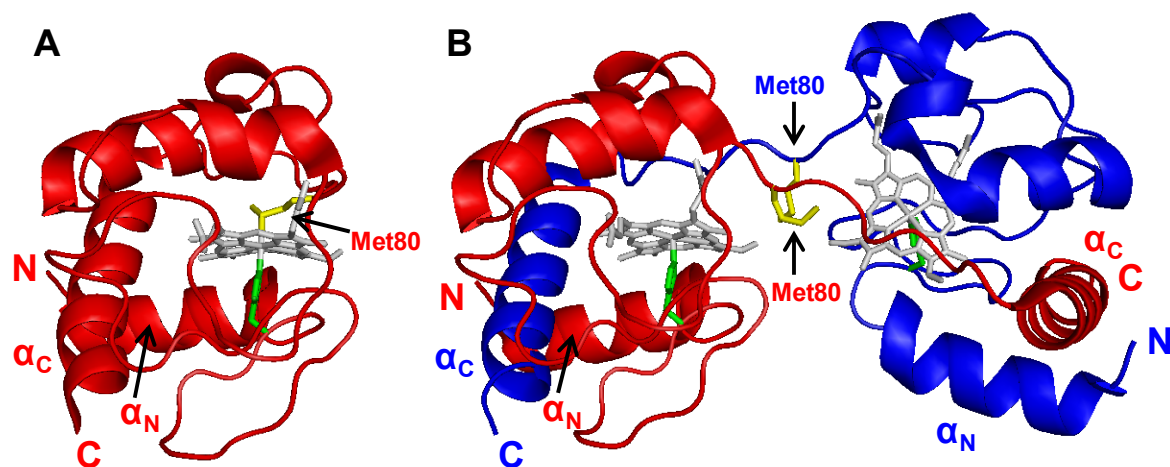


Figure 1

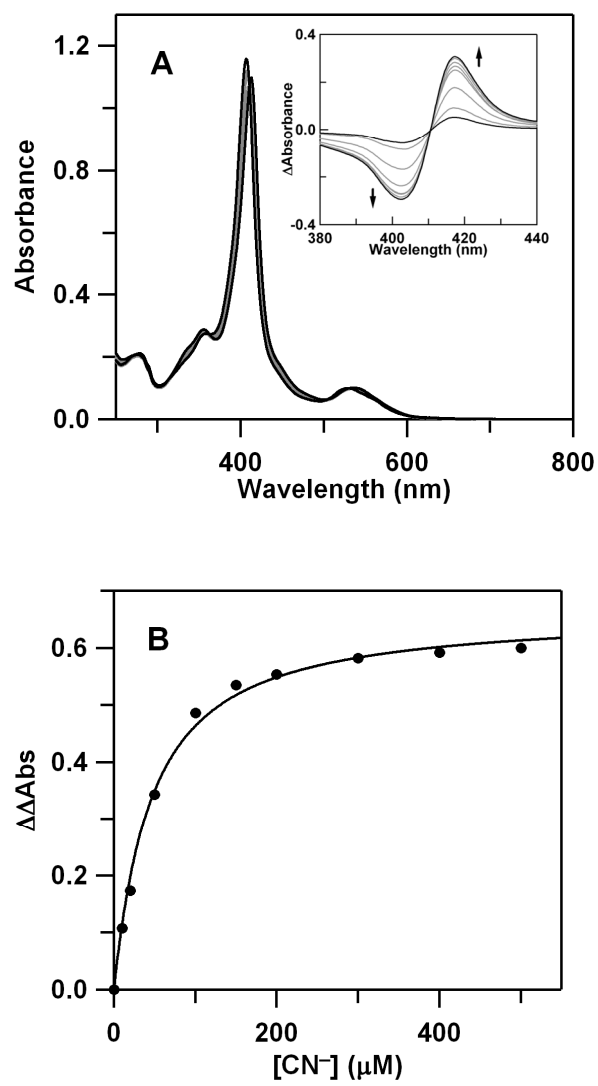


Figure 2

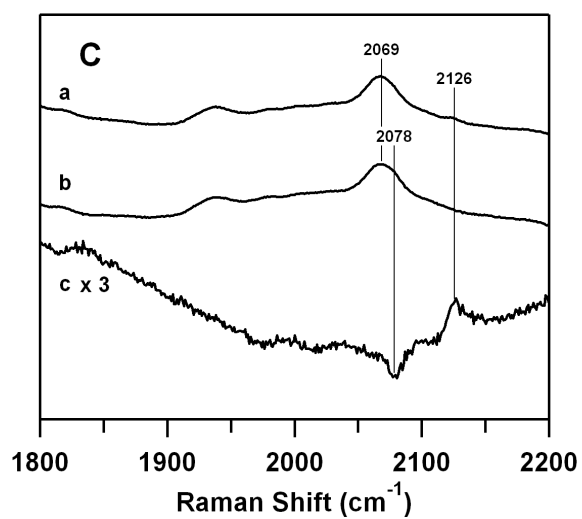
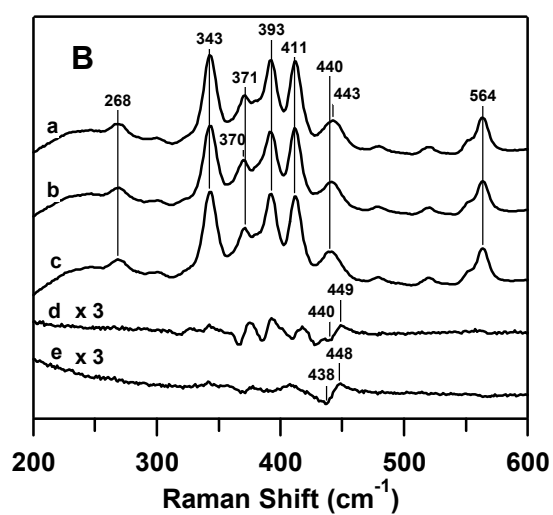
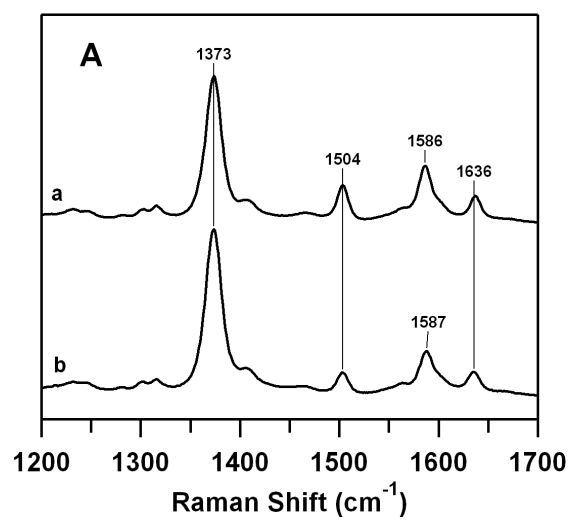


Figure 3

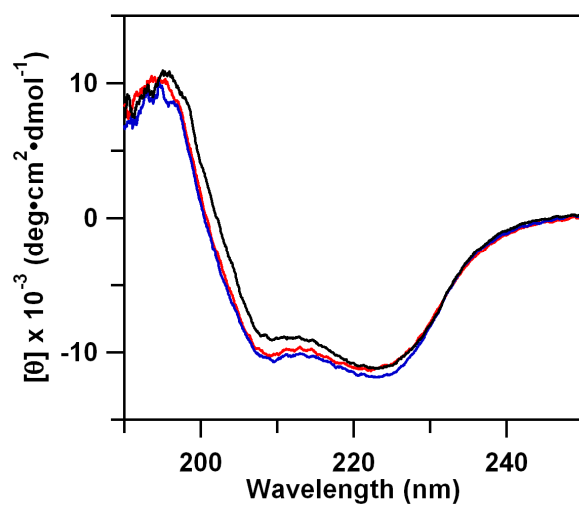


Figure 4

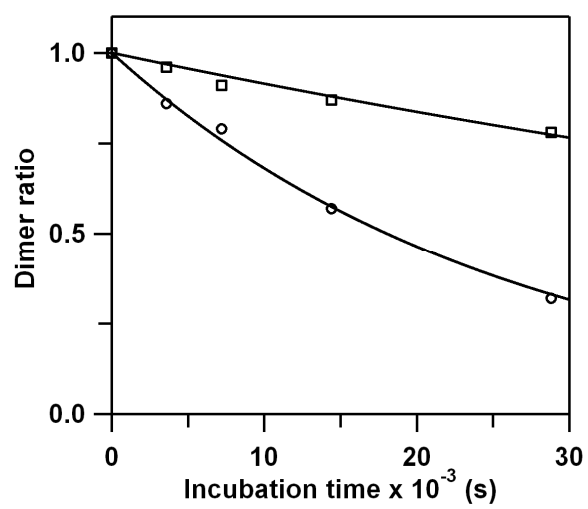


Figure 5



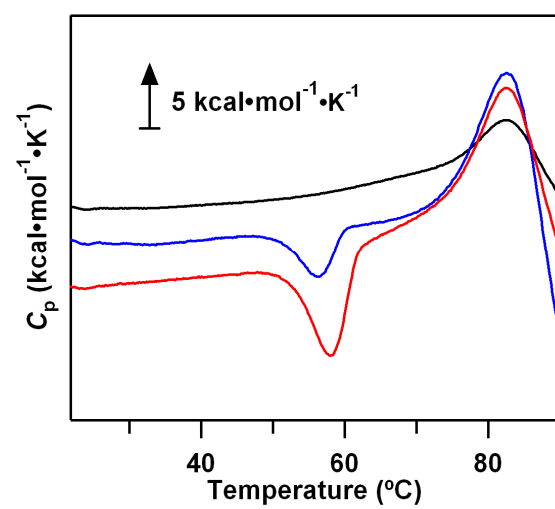


Figure 6

# Interaction of dimeric horse cytochrome *c* with cyanide ion

Ari Dwi Nugraheni<sup>a</sup>, Satoshi Nagao<sup>a</sup>, Sachiko Yanagisawa<sup>b</sup>, Takashi Ogura<sup>b</sup>, and Shun Hirota<sup>\*,a</sup>

<sup>a</sup> Graduate School of Materials Science, Nara Institute of Science and Technology,  
8916-5 Takayama, Ikoma, Nara 630-0192, Japan

<sup>b</sup> Graduate School of Life Science, University of Hyogo, Koto 3-2-1, Kamigori  
Ako, Hyogo 678-1297, Japan

## Contents

<b>Fig. S1</b>	Optical absorption spectra in the Q-band region of oxidized dimeric horse cyt <i>c</i> .	p.2
<b>Fig. S2</b>	Absorption spectra of oxidized monomeric horse cyt <i>c</i> .	p. 3
<b>Fig. S3</b>	Absorption spectrum of cyt <i>c</i> after dissociation of oxidized dimeric horse cyt <i>c</i> .	p. 4

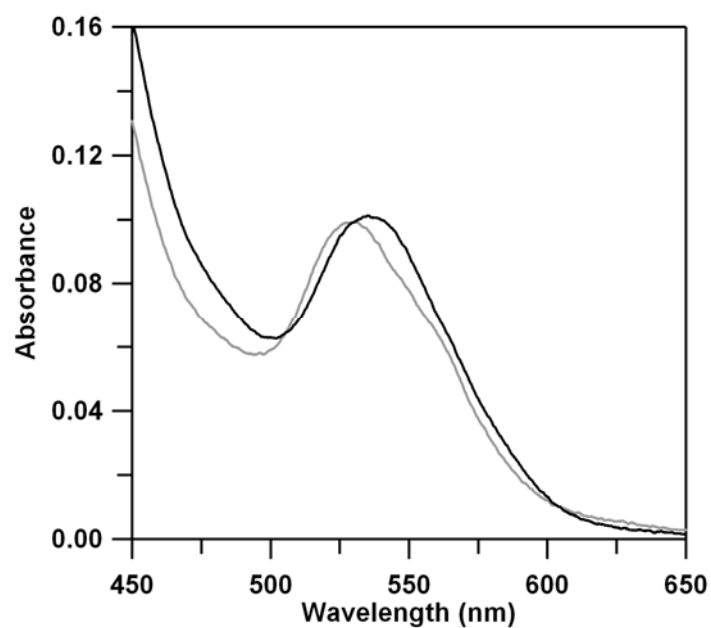


**Fig. S1** Optical absorption spectra in the Q-band region of oxidized dimeric horse cyt *c* in the presence (black) and absence (gray) of cyanide ion. Measurement conditions: dimeric cyt *c* concentration (heme unit): 10  $\mu$ M, KCN concentration: 0 (gray) and 0.5 (black) mM, solvent: 50 mM potassium phosphate buffer, pH 7.0, temperature: 20  $^{\circ}$ C.

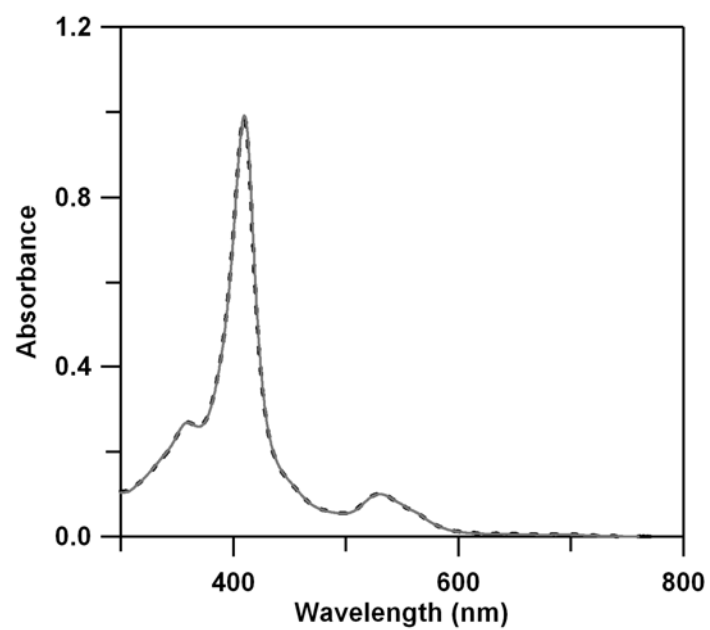


**Fig. S2** Absorption spectra of oxidized monomeric horse cyt *c* in the presence (dashed line) and absence (solid gray line) of cyanide ion. Measurement conditions: monomeric cyt *c* concentration: 10  $\mu$ M, KCN concentration: 1 mM, solvent: 50 mM potassium phosphate buffer, pH 7.0, temperature: 20  $^{\circ}$ C.

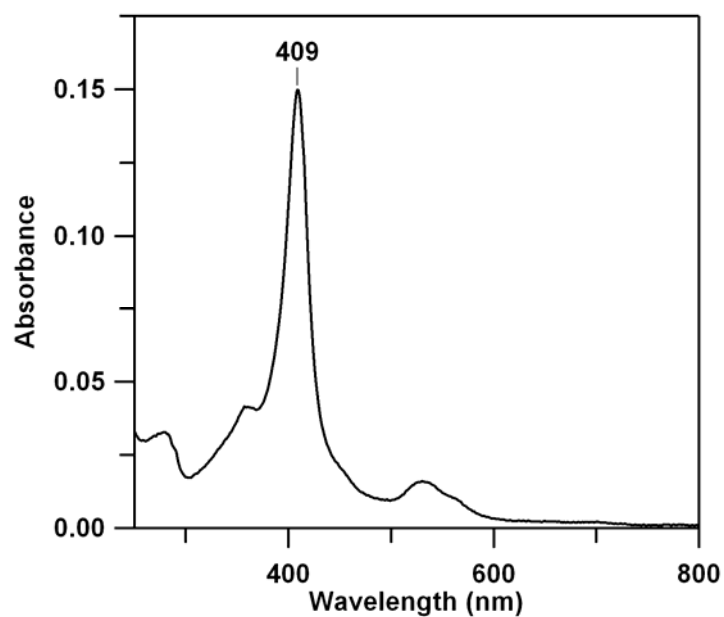


**Fig. S3** Absorption spectrum of cyt *c* after dissociation of oxidized dimeric horse cyt *c* in the presence of cyanide ion. Dimeric cyt *c* with 1 mM cyanide ion was incubated at 45 °C for 8 hr and purified by gel filtration. Measurement conditions: cyt *c* concentration (heme unit): ~1.5  $\mu$ M, solvent: 50 mM potassium phosphate buffer, pH 7.0, temperature: 20 °C.